# Three-Dimensional Tubular Impact Energy Absorber

**A. A. A. Alghamdi**
Department of Mechanical Engineering, King Abdulaziz University
Jeddah 21589, Saudi Arabia
Fax 966-2-695-2193
Email: aljinaidi@hotmail.com

**Abstract**

This paper presents an innovative three-dimensional collapsible impact energy absorber. The absorber consists of twelve thin tubes welded together to form a cubic cell. When crushed between two parallel plates, the vertical tubes deform axially while the horizontal ones deform laterally. Energy is absorbed in the plastic buckling of longitudinal tubes and plastic flattening of the transverse ones. Quasi-static experimental investigations were carried out for absorbers made of low-carbon steel using 30-Ton Universal Instron Testing Machine. Obtained results clearly illustrate the interactions between the two modes of deformation as well as the relative high specific energy of the absorber.

## INTRODUCTION

With the increase in speed of the transportation system, researchers have been looking for ways to minimize serous damage during impact and crash events. Plastic deformation of thin metallic structures has been used as impact energy absorbers for decades now. The kinetic energy of the impacted body is dissipated in the absorber in an irreversible process through a sequence of plastic deformation work.

Energy absorbers are used in daily life. Typical example is car bumper that has a primary function of absorbing a collision in a proper manner. A plastic permanent damage to the bumper is highly wanted in an attempt to absorb the kinetic energy of the moving automobile or the kinetic energy of the impacted one. This deformation in the bumper will reduce the deceleration pulse felt by the passenger, thus reducing the risk of the impact.

There have been so many collapsible devices in the literature. Some of the well-known absorber devices include, circular tubes [Reid, 1993], frusta [Mamalis and Johnson, 1983], honeycomb structures [Wu and Jiang, 1997], square tubes [Langseth and Hopperstand, 1996], cubic rod cell [Alghamdi, 2000] and so on, see [Alghamdi, 2001].

Thin circular tubes have been used as impact energy absorbers since the pioneering work of Alexander [Alexander, 1960]. Since then, researchers have used circular tubes in different deformation modes including, axial crushing [Johnson et al., 1977], tearing and splitting [Stronge et al., 1984], nosing [Reid and Harrigan, 1998], inversion [Al-Hassani et al., 1972], lateral (flattening) loading [Deruntz and Hodge, 1963] and lateral indentation [Watson, et al., 1976]. Efforts to use hybrid absorbers lead to axial crushing of wood-filled square metal tubes [Reddy and Al-Hassani, 1993], axial compression of foam-filled circular tubes [Reddy and Wall, 1988] and others [Johnson and Reid, 1978]. In these mechanisms the absorption is made in an irreversible manner and the structure is deformed plastically Axial crushing of thin tubes provides one of the best energy absorber because of their common existence as structural elements in addition to their high-energy capacity that can reach up to 30J/g for low carbon steel [Jones, 1989]. This optimum absorption can be obtained by progressive plastic buckling which avoids overall elastic buckling. Thus, only short cylinders are used as energy absorbers where long ones suffer from the global elastic buckling with very limited energy absorption. So far, there is no way to get progressive plastic buckling (crumpling) for long columns under static or dynamic testing conditions. A major drawback of axial crushing is the directional sensitivity of the load. This means if the load is not concentric with axis of the tube, then the crushing mode is not uniform, not predictable and not even reported in the literature.

Lateral crushing of thin tube provides stable crushing mode with relatively insensitive to the direction of loading but with energy absorption capacity one order of magnitude less than the axial mode. However, specific energy is still much better than the specific energy in lateral indentation where the deformation is localized phenomenon. Systems made of thin tubes crushed laterally have been studied by many researchers, see for example [Reddy and Reid, 1979], [Reddy et al., 1987] and [Wu and Carney, 1998].

Reid et al. [1984] described the mode of deformation and the behavior of a two-dimensional tubular ring under static and dynamic loads. Each square ring consisted of four sections of tube cut at 45° welded together. The obtained results showed remarkable increase in energy absorbing capacity over equivalent free tube crushed laterally. This is attributed to the integrity of the ring, where more energy is dissipated at the four welded joints. The paper is summarized by stating that the tubular ring provides an efficient way of improving the energy absorbing capacity of circular metal tubes without utilizing external source of constraint.

In this paper effort made by Reid et al. [1984] to build two-dimensional tubular ring is extended to build three-dimensional tubular cubic cell. Thus an innovative system of impact energy absorber is presented. The system is made of low carbon steel tubes welded together to form a cubic cell. Load displacement curves showing the characteristics of the proposed system under static loading condition are given for absorbers with different diameters and different sizes.

## THE ABSORBER

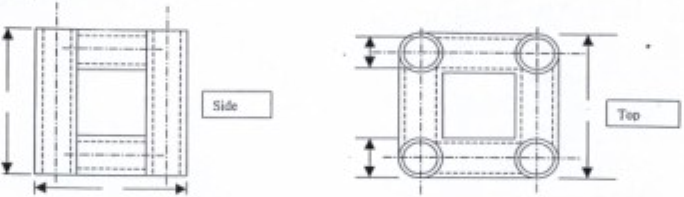


Figure 1: Schematic Drawing of the Three-Dimensional Tubular Absorber.

Figure 1 shows the proposed system of absorber that consists of four vertical tubes joined together by eight horizontal tubes. All of these tubes have the same outer diameter (D), inner diameter (d) and wall thickness (t). Length of the vertical tubes is L while the horizontal ones are shorter by two times the outer diameter (D), as shown in Figure 1 (note: front view is identical to the shown side view). The aspect ratio (R) is defined as the ratio between the side length (L) and the outer diameter (D). Tens of absorbers made of low carbon steel were manufactured with different outer diameters and different aspect ratios; see Figure 2 and Table 1.

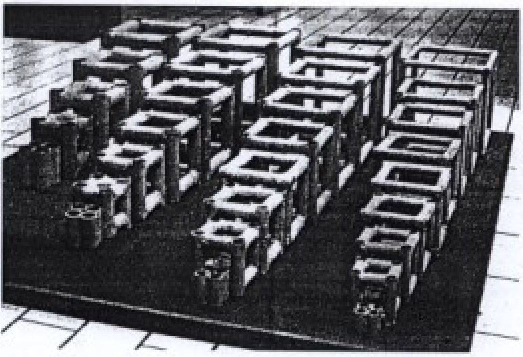

Figure 2: Three-Dimensional Tubular Absorbers before Crushing Tests

Absorbers were manufactured from the same set of tubes to insure uniformity in the material with yield strength equals to 385 MPa. They were grouped into four groups depending on their outer diameters, as shown in Table 1.

A series of quasi-static tests were carried out using a 30-Ton Universal Instron Testing Machine. A loading rate of 5 mm/min was maintained throughout these tests.

## RESULTS AND DISCUSSION

Details of the load-displacement curve for crushing the tubular absorber is shown in Figure 3. In this figure the load (in kN) is plotted against the displacement (in mm) for Specimen 2504, see Table 1 for the dimensions of this specimen. The average crushing force is found to be 169.3 kN whereas the energy absorbed (area under the curve) is calculated by multiplying the average force by the maximum displacement to give 11530 J. The corresponding specific energy is 17.04 J/g. See Table 1. Five photograph frames taken during crushing test at

Table 1: Dimensions of the Specimens used and Details of the Experimental Work.

| No. | Sp. No. | D (mm) | d (mm) | t (mm) | L (mm) | Aspect Ratio (R=L/D) | Mass (g) | Initial Force (kN) | Average Force (kN) | Energy (J) | Specific Energy (J/g) |
|---|---|---|---|---|---|---|---|---|---|---|---|
| 1 | 2002 | 20 | 17 | 1.5 | 40 | 2 | 109.5 | 165 | 148.8 | 3719 | 33.97 |
| 2 | 2004 | 20 | 17 | 1.5 | 80 | 4 | 438.0 | 132 | 124.8 | 7176 | 16.38 |
| 3 | 2005 | 20 | 17 | 1.5 | 100 | 5 | 602.2 | 135 | 120 | 9300 | 15.44 |
| 4 | 2006 | 20 | 17 | 1.5 | 120 | 6 | 766.5 | 81 | 52.57 | 5257 | 6.859 (stopped) |
| 5 | 2007 | 20 | 17 | 1.5 | 140 | 7 | 930.7 | 131 | 62.58 | 7197 | 7.733 |
| 6 | 2008 | 20 | 17 | 1.5 | 160 | 8 | 1095 | 133 | 74.39 | 10040 | 9.171 |
| 7 | 2009 | 20 | 17 | 1.5 | 180 | 9 | 1259 | 126 | 46.06 | 7139 | 5.671 |
| 8 | 2502 | 25 | 22 | 1.5 | 50 | 2 | 173.9 | 230 | 191.5 | 6704 | 38.55 |
| 9 | 2504 | 25 | 22 | 1.5 | 100 | 4 | 695.4 | 205 | 169.3 | 11850 | 17.04 |
| 10 | 2505 | 25 | 22 | 1.5 | 125 | 5 | 956.2 | 190 | 128.1 | 11530 | 12.06 |
| 11 | 2506 | 25 | 22 | 1.5 | 150 | 6 | 1217 | 185 | 107.2 | 12320 | 10.13 |
| 12 | 2507 | 25 | 22 | 1.5 | 175 | 7 | 1478 | 182 | 86.34 | 12090 | 8.18 |
| 13 | 2508 | 25 | 22 | 1.5 | 200 | 8 | 1739 | 178 | 42.47 | 6795 | 3.908 |
| 14 | 2509 | 25 | 22 | 1.5 | 225 | 9 | 1999 | 145 | 47.26 | 8507 | 4.256 |
| 15 | 2510 | 25 | 22 | 1.5 | 250 | 10 | 2260 | 110 | 35.09 | 7719 | 3.415 |
| 16 | 3202 | 32 | 29 | 1.5 | 64 | 2 | 288 | 247 | 177.7 | 8438 | 29.22 |
| 17 | 3203 | 32 | 29 | 1.5 | 96 | 3 | 722.1 | 225 | 194.1 | 12620 | 17.47 |
| 18 | 3204 | 32 | 29 | 1.5 | 128 | 4 | 1155 | 220 | 180.2 | 14420 | 12.48 |
| 19 | 3205 | 32 | 29 | 1.5 | 160 | 5 | 1589 | 218 | 169.3 | 18620 | 11.72 |
| 20 | 3206 | 32 | 29 | 1.5 | 192 | 6 | 2022 | 235 | 88.9 | 12890 | 6.375 |
| 21 | 3207 | 32 | 29 | 1.5 | 224 | 7 | 2455 | 210 | 74.11 | 13340 | 5.433 |
| 22 | 3208 | 32 | 29 | 1.5 | 256 | 8 | 2888 | 212 | 65.57 | 13110 | 4.541 |
| 23 | 4202 | 42 | 39 | 1.5 | 84 | 2 | 503.3 | 265 | 183.7 | 10560 | 20.98 |
| 24 | 4203 | 42 | 39 | 1.5 | 126 | 3 | 1258 | 227 | 180.8 | 16280 | 12.94 |
| 25 | 4204 | 42 | 39 | 1.5 | 168 | 4 | 2014 | 255 | 183.4 | 22000 | 10.93 |
| 26 | 4205 | 42 | 39 | 1.5 | 210 | 5 | 2769 | 260 | 170.6 | 25580 | 9.239 |

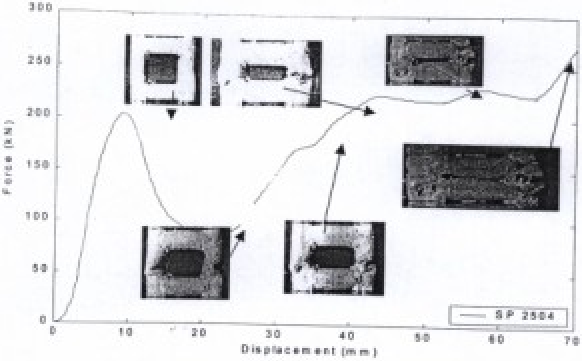


Figure 3: Load Displacement Curve for Specimen 2504.

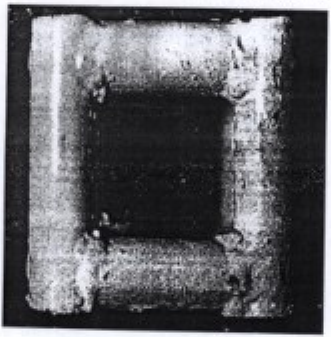

different intervals are shown in Figure 3, while photographs of the specimen before and after the test are shown in Figure 4. The test starts at origin and the load increases at low rate in the first few millimeters because the cell is not fully loaded yet due to the expected distortion of the cell during welding. Then the load increases sharply to a peak value. This value represents instability point. At this point (point a) a first frame was shot at 10-mm displacement and it is shown in the figure. The progressive plastic buckling of the longitudinal tubes starts at point a. The deformation mode seen here is diamond asymmetric mode with two lobes. Another frame was taken at 20-mm displacement. It shows clearly the asymmetric deformation of the longitudinal tubes. Note that although the horizontal tubes are not deformed yet, the eight joints undergo plastic deformation. In another words, at this stage the horizontal tubes provide boundary constrains for the axial ones and hence undergo some localized deformation. Point b in the curve represents the lowest crushing load in the whole curve that is corresponding to the end of collapsing of the first convolution of the vertical tubes. Also, it was noticed that the progressive collapse starts at either the upper or the lower sides of the vertical tubes and there was no general pattern regarding this distribution. Another frames were captured at 30 and 40-mm displacement while the load is increasing due to the resistance of the second convolution formation. Because of the short vertical tubes, the second convolution in the vertical tubes did not go through independently and deformation extends into the eight joints as shown in the frame taken at 56-mm displacement. Interaction between the axial crushing of the four vertical tubes and lateral flattening of the eight horizontal tubes started after approximately 40-mm of displacement. The progressive crumpling of the vertical tubes continues while indirect lateral deformation of the horizontal tubes takes place after 40-mm displacement. It is indirect flattening because there is no direct touch between opposite horizontal tubes and the flattening is achieved through the eight joints. This indirect flattening is shown in the frame taken at 56-mm displacement. At 64-mm displacement the upper horizontal tubes touche the lower ones causing a sudden increase in the load. The test stopped after 70.64-mm at which the maximum permissible load in the machine is reached.

**Aspect Ratio Effect**

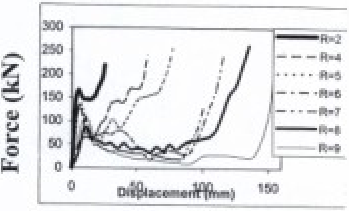


Figure 5: Load-Displacement Curves for Specimens 2002 Through 2009.

Cells with different aspect ratios but same outer diameter were tested as given in Table 1. Typical set of curves is given in Figure 5 for the first group in Table 1, i.e. D=20 mm group. The first thing to notice is as the aspect ratio increases, the absorber size increases and the crushing distance increases too. As the aspect ratio is increased, the plastic deformation pattern changed from progressive plastic crumpling into global plastic bending with one plastic bending hinge in the vertical tubes, thus they have less participation in absorption mechanism. So, the mean average force decreases with the increase in the aspect ratio leading to less tube efficiency, i.e. less specific energy. In all tested cases the load increases to some initial peak and then decreases till the upper horizontal tubes touches the lower ones. Between the initial peak and the second increase in the load, there is no general trend in the behavior of the curve. However, this zone is very much affected by the progressive collapse of the longitudinal tubes. So, you could see variation in the load due to the successive collapse of the vertical tubes for small aspect ratio (like R=5), but steadier decreasing load for large aspect ratio (like R=9), where global plastic buckling at localized hinge in the middle of vertical tubes dominates the deformation mode. One can see clearly that the best aspect ratio is R=2 which is corresponding to the case of having four vertical tubes welded together. But, this maximum energy capacity is obtained for axial crushing mode between two parallel plates. In another words, different loading conditions, like point loading, line loading or loading between non-parallel plates, may give different results. Also, from practical point of view, closed compact absorber may not be the right choice. To give an example consider the case of metal absorber suggested to be installed between highway concrete bridges and mountains in Saudi Arabia where these devices work to absorb the kinetic energy of falling rocks from the nearby mountain [Alghamdi, 2000]. Absorber with aspect ratio R=2 means that the absorber will block the way of falling particles, sands, loose stones, and hence loosing its function.

The relation between maximum instability force and aspect ratio is shown in Figure 6. As expected, the instability force increases with the increase in the cross sectional area of the tubular cell, but decreases with the increase in the aspect ratio due to global buckling effect. Large aspect ratio means large cell with long vertical tubes willing to collapse into Euler buckling mode.

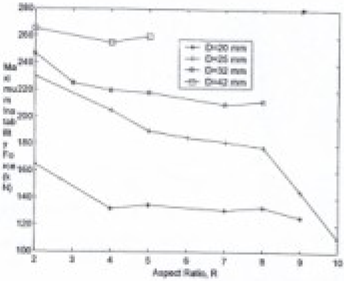


Figure 6: Relation Between Maximum Instability Force and Aspect Ratio.

**Tube Diameter Effect**

Figure 7 shows load-deformation curves for cells with the same aspect ratio (R=2), but different outer diameters. The general trend is the same in these curves and, as expected, the average crushing force increases with the increase in tube diameter. However, specific energy attains high value for D=25 mm. Good thing to notice is the square wave pattern of the loading curve. This type of pattern is highly wanted in designing impact energy absorber because it provides constant deceleration wave to the passengers or the vehicle itself. The uniformity in the load after the initial peak is attributed to the interactions between the progressive plastic buckling of the four tubes. Thus, progressive collapses in these four tubes were not simultaneous. In other words, due to welding, tubes were not behaving independently and yet were not following each other in crumpling sequences. So, the overall response is uniform whereas single tube show fluctuating load pattern, see [Reid, 1993].

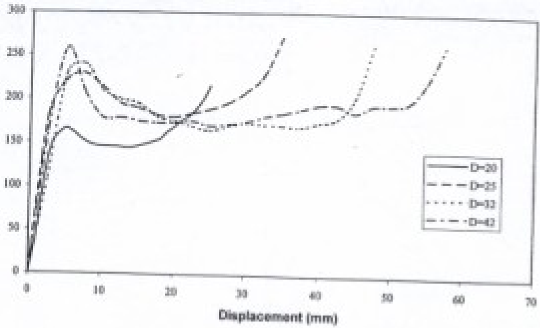


Figure 7: Load-Displacement Curves for Specimens 2002, 2502,3202 and 4202.

**Specific Energy**

Specific energy for each specimen is given in the last column of Table 1. However, relations between specific energy, as a measure of device efficiency, and aspect ratio as well as other deformation modes are given in Figures 8-10.

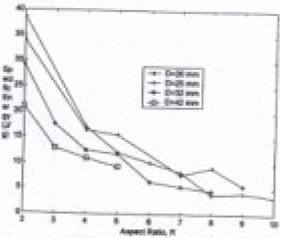


Figure 8: Relation Between Specific Energy and Aspect Ratio.

In Figure 8 the specific energy (in J/g) is plotted vs. aspect ratio for the four diameters tested in this paper. General speaking, tubes with small diameters are more efficient when compared to large ones.

Figure 9 is plotted in an attempt to look for an optimum aspect ratio. One can select aspect ratio R=5 as an optimum value because of the higher volume-energy value at this ratio for three sizes out of four. Again this might not be agreeing upon selection criteria, but it was chosen for optimum aspect ratio for the falling rock project discussed above [Alghamdi, 2000].

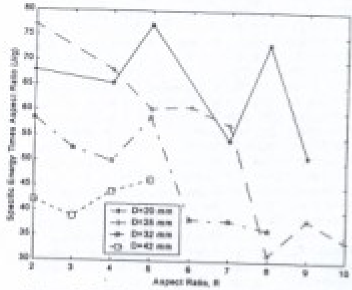


Figure 9: Specific Energy Times Aspect Ratio vs. Aspect Ratio.

In Figure 10, maximum specific energy of the suggested tubular absorber is compared to the maximum specific energy for other modes of deformation [Jones, 1989]. Although, only the maximum value is being compared here, the suggested device is a promising absorber. This tubular absorber has some clear advantages over other devices such as; all metal participates in the deformation when compared to other modes such as tube inversion or tube flattening and less directional sensitivity when compared to axial crushing of single tube or tube expansion or tension.

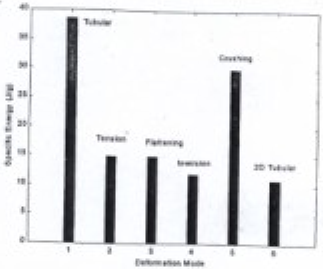


Figure 10: Specific Energy for Tubes Under Deferent Modes of Deformation.

## CONCLUDING REMARKS

In this paper an innovative collapsible impact energy absorber in the form of three-dimensional tubular system is introduced. The absorber consists of twelve tubes welded to together to form a cubic cell. When crushed axially between two parallel plates energy is dissipated in crushing axial tubes first then flattening of horizontal tubes. Absorbers with small aspect ratio give high specific energy with maximum value at R=2 because of the progressive plastic buckling of longitudinal tubes and the absence of global plastic buckling. Maximum specific energy obtained experimentally is 38 J/g for absorber made of 25-mm tube diameter and aspect ratio R=2. The load-displacement curves for small aspect ratio have an excellent shape from impact energy consideration. Further investigation of other loading modes such as crushing between non-parallel plates is expected to show better performance of this absorber when compared to other absorbers especially in the domain of load directional sensitivity and stability of the system.

## ACKNOWLEDGEMENT

The author would like to acknowledge King Abdulaziz University for their support of this work through my sabbatical leave grant during 2001/2002 academic year. Help provided by Mr. A. Riri in specimens' preparation is highly appreciated.

## REFERENCES

1. Alexander, J. M., An Approximate Analysis of the Collapse of Thin Cylindrical Shells Under Axial Loading, *Quarterly Journal of Mechanics and Applied Mathematics*, 13 (1), pp. 10-15, 1960.

2. Alghamdi, A. A. A., Protection of Saudi Descent Roads using Metallic Collapsible Energy Absorbers, Final Report Submitted to KACST, Riyadh, Saudi Arabia, Grant Number 98-2-74, April 2000.

3. Alghamdi, A. A. A., Collapsible Energy Absorbers: An Overview, *Thin-Walled Structures*, 39, pp. 189-213, 2001.

4. Al-Hassani, S. T. S., Johnson, W. and Lowe, W. T., Characteristics of Inversion Tube Under Axial Loading, *Journal of Mechanical Engineering Science*, 14, pp. 370-381, 1972.

5. Deruntz, J. A. and Hodge, P. G., Crushing of a Tube Between Rigid Plates, *Journal of Applied Mechanics*, 30, pp. 391-398, 1963.

6. Johnson, W. and Reid, S. R., Metallic Energy Dissipating Systems, *Applied Mechanics Review*, 31 (3), pp. 277-288, 1978.

7. Johnson, W., Soden, P. D. and Al-Hassani, S. T. S., Inextensional Collapse of Thin-Walled Tubes Under Axial Compression, *Journal of Strain Analysis*, 12, pp. 317-330, 1977.

8. Jones, N., Structural Impact, Cambridge University Press, Cambridge, 1989.

9. Langseth, M. and Hopperstand, O. S., Static and Dynamic Axial Crushing of Square Thin-Walled Aluminum Extrusions, *International Journal of Impact Engineering*, 18 (7/8), pp. 949-968, 1996.

10. Mamalis, W. and Johnson, W., The Quasi-Static Crumpling of Thin-Walled Circular Cylinders and Frusta Under Axial Compression, *International Journal of Mechanical Science*, 25 (9/10), pp. 713-732, 1983.

11. Reddy, T. Y. and Al-Hassani, S. T. S., Axial Crushing of Wood-Filled Square Metal Tubes, *International Journal of Mechanical Science*, 35 (3/4), pp. 231-246, 1993.

12. Reddy, T. Y. and Reid, S. R., Lateral Compression of Tubes and Tube-Systems with Side Constraints, *International Journal of Mechanical Science*, 21, pp. 187-199, 1979.

13. Reddy, T. Y., Reid, S. R., Carney, J. F. and Veillette, J. R., Crushing Analysis of Braced Metal Rings Using the Equivalent Structure Technique, *International Journal of Mechanical Science*, 29 (9), pp. 655-668, 1987.

14. Reddy, T. Y. and Wall, R. J., Axial Compression of Foam-Filled Thin-Walled Circular Tubes, *International Journal of Impact Engineering*, 7, pp. 151-160, 1988.

15. Reid, S. R., Plastic Deformation Mechanisms in Axially Compressed Metal Tubes used as Impact Energy Absorbers, *International Journal of Mechanical Science*, 35 (12), pp. 1035-1052, 1993.

16. Reid, S. R., Austin, C. D. and Smith, R., Tubular Rings as Impact Energy Absorber, In Structural Impact and Crashworthiness, Davies, G. and Morton, J. (Eds.), Elsevier, New York, pp. 555-563, 1984.

17. Reid, S. R. and Harrigan, J. J., Transient Effects in the Quasi-Static and Dynamic Internal Inversion and Nosing of Metal Tubes, *International Journal of Mechanical Science*, 40 (2/3), pp. 263-280, 1998.

18. Stronge, W. J., Yu, T. X. and Johnson, W., Long Stroke Energy Dissipation in Splitting Tubes, *International Journal of Mechanical Science*, 25, pp. 637-647, 1984.

19. Watson, A. R., Reid, S. R., Johnson, W. and Thomas, S. G., Large Deformation of Thin-Walled Circular Tubes Under Transverse Loading, *International Journal of Mechanical Science*, 18 (5), pp. 387-398, 1976.

20. Wu, E. and Jiang, W-S., Axial Crush of Metallic Honeycombs, *International Journal of Impact Engineering*, 19 (5/6), pp. 439-456, 1997.

21. Wu, L. and Carney III, J. F., Experimental Analysis of Collapse Behaviors of Braced Elliptical Tubes Under Lateral Compression, *International Journal of Mechanical Science*, 40 (8), pp. 761-777, 1998.